High-Contrast Plasma-Electrode Pockels Cell (PEPC)

Introduction

Many high-energy laser systems under development for inertial confinement fusion (ICF) use a multipass amplifier architecture.[1,2] A large-aperture optical switch, which is capable of withstanding high fluence, is often utilized in these systems to control the number of passes that a laser pulse makes through the amplifier cavity. Conventional Pockels cells that use ring electrodes cannot be scaled to the large apertures required for ICF lasers. Therefore, the plasma-electrode Pockels cell (PEPC) technology, which uses high-conductivity plasmas as electrodes, was developed at Lawrence Livermore National Laboratory (LLNL) for use in ICF laser systems.[3–6]

Most existing multipass high-energy laser systems use frequency conversion to direct second- or third-harmonic light onto the target. This is not the case, however, for the high-energy petawatt-class laser system that is being constructed on OMEGA EP at the Laboratory for Laser Energetics.[1] In this short-pulse system, the light is not frequency converted before being sent to the target. Any light reflected by the target can therefore experience gain as it propagates back up the system. Because the amplifiers are unsaturated, a retroreflected pulse can experience high gain, posing a significant threat of system damage. Isolation of the amplifier cavity from back-reflected light is, therefore, required on this system.

In addition to the more typical role of holding the pulse in the cavity for four passes, the OMEGA EP PEPC will be used to provide isolation from target retroreflections. This concept is illustrated in Fig. 107.1. Figure 107.1(a) shows a block diagram of a portion of the OMEGA EP Laser System; Fig. 107.1(b) is a timing diagram showing the state of the PEPC switch. The pulse from the laser sources area is injected into the beamline at the transport spatial filter (TSF) at time T and enters the
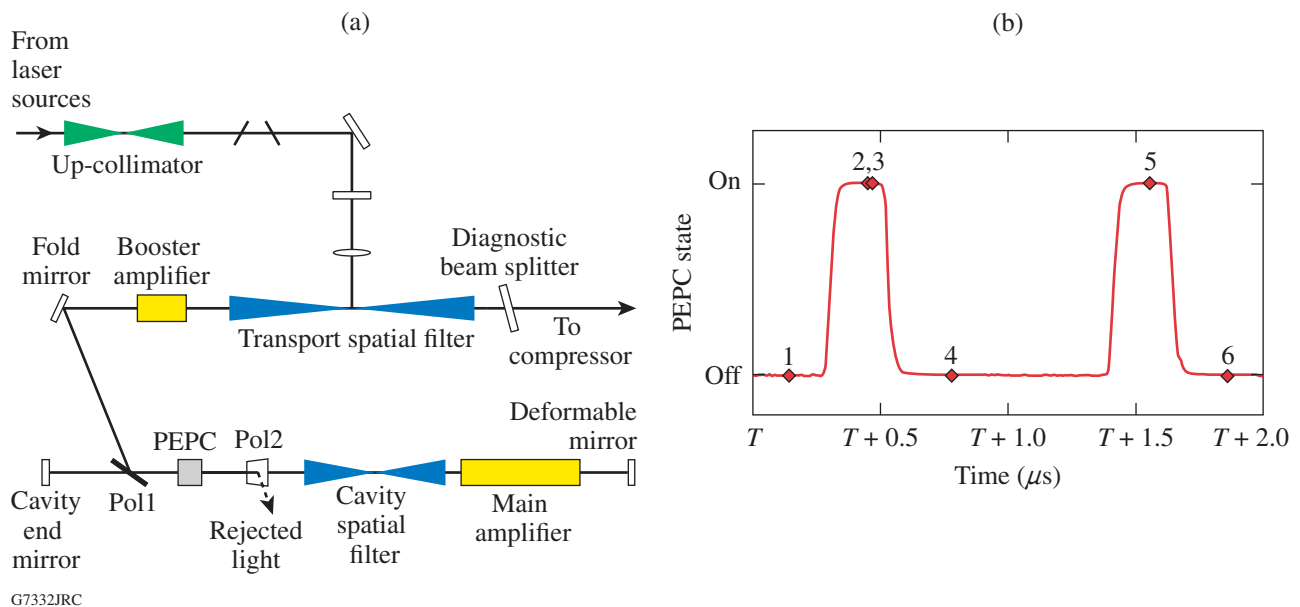

Figure 107.1
(a) Diagram of the OMEGA EP Laser System showing the PEPC in relation to key beamline components. (b) Timing diagram showing the state of the PEPC as a function of time. Times during which the laser pulse passes through the PEPC are highlighted.

amplifier cavity by reflecting from the cavity polarizer. The pulse makes Pass 1 through the PEPC while the PEPC is in its unenergized state. The pulse is amplified by two passes through the main amplifier chain before returning for Pass 2 through the PEPC, which will then be switched to its active state. This allows the laser pulse to remain in the amplifier cavity for two more passes. At Pass 4, the PEPC is again unenergized to couple the pulse out of the amplifier cavity, from which it is transported to the target chamber. Approximately 700 ns later, the retroreflected pulse couples back into the amplifier cavity for Pass 5 through the PEPC. The PEPC must be energized at this time to switch the retroreflected pulse out of the cavity to a beam dump via a polarizer labeled Pol 2 in Fig. 107.1(a). Any residual light that is not switched out of the cavity will be reamplified; therefore, the PEPC must be in the unenergized state upon its return at Pass 6 to ensure that the light is not trapped in the cavity and further amplified.

This new role of providing isolation places greater demands on the switching contrast ratio (the ratio of maximum transmission to minimum transmission of the PEPC between two ideal polarizers). To control the amplified passes through the cavity (Passes 1 through 4), the PEPC is required to provide a contrast of >100:1 averaged over the clear aperture, or >50:1 locally. To provide sufficient isolation on the OMEGA EP system for Passes 5 and 6, however, the PEPC is required to switch with a contrast ratio exceeding 500:1 locally, i.e., at all points in the clear aperture.

This requirement exceeds the performance reported on existing PEPC cells, which are typically limited to approximately 100:1 locally, primarily due to stress-induced birefringence in the vacuum-loaded windows.[5,7] This article describes a redesigned PEPC that achieves a significantly higher contrast. It addresses the development of a window geometry that exhibits low stress-induced birefringence required to increase contrast and presents observations of a PEPC switching contrast ratio that reliably exceeds the 500:1 requirement.

High-Contrast PEPC Design

The prototype PEPC cell, seen in operation in Fig. 107.2, was built to evaluate design concepts for increasing the switching contrast. A cross-sectional sketch of the system (Fig. 107.3) highlights the main features of the PEPC cell. The design was based on the LLNL PEPC in use by the National Ignition Facility (NIF) and was repackaged for use in a single-beam configuration.[7] The main structural components, the two halves of the cell body, are made of aluminum and are anodized to provide a dielectric barrier from the plasma. Sandwiched between the cell
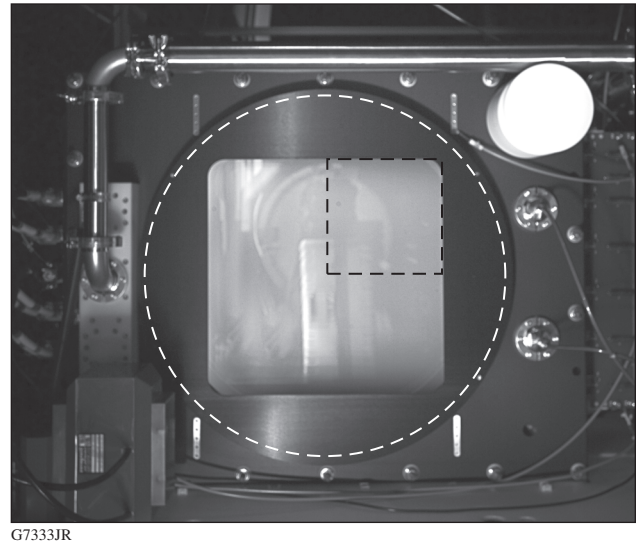

G7333JR

Figure 107.2
Photograph of the prototype PEPC during plasma ignition. The outline of the windows is indicated by the white dashed circle, and the region analyzed by the stress birefringence model is indicated by the black dashed square.

body halves is a glass midplane, with the electro-optic crystal potted in the center using an aerospace silicone epoxy. The electro-optic crystal is a $40 \times 40 \times 1$-cm plate of Z-cut KDP grown via the rapid-growth method at LLNL.[8] Fused-silica windows, which will be discussed in more detail in **Reduction of Window Stress Birefringence** (p. 131), are mounted on the cell body. These windows are circular, as indicated by the white dashed line in Fig. 107.2.

The plasma electrodes are formed in two chambers between the glass midplane and the windows. The cell is evacuated using a turbomolecular pump and back-filled with helium to 80 mT. Graphite electrodes are mounted on either end of the plasma cavity. The anodes are segmented into six button-type electrodes and the cathodes are planar magnetrons. A simmer discharge is initiated by breaking down the gas between the cathode and a nearby starter anode rod. A low-density discharge is maintained across the plasma channel for 450 ms. Near the end of the simmer discharge, a 10-μs, 4-kV pulse is applied, which increases the plasma density to $>10^{12}$ cm^{-3} to create high-conductivity electrodes.[9] When the plasma is in this high-conductivity state, a 250-ns, 18-kV switch pulse applied between the plasmas produces the electric field necessary to impart a half-wave retardance on the 1053-nm incident beam. The electrode size produces a plasma channel that is 8 cm wider than the vertical extent of the clear aperture, thereby mitigating the effects of plasma pinching.[10,11]
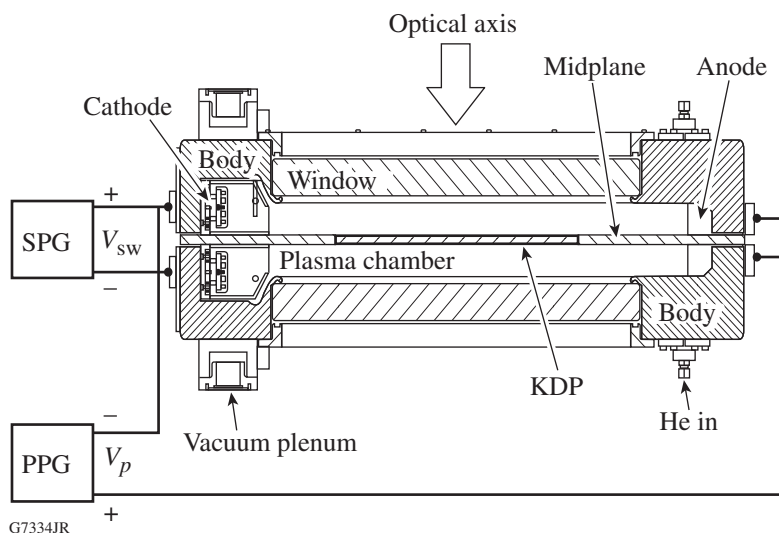
130

Figure 107.3
Cross-sectional view of the PEPC cell showing the key elements of the PEPC system. SPG denotes the switch pulse generator, and PPG indicates two plasma pulse generators.

Reduction of Window Stress Birefringence

The primary contrast limitation in the NIF PEPC cell design is the stress-induced birefringence in the square windows that form the air-vacuum barrier for the plasma. To achieve the contrast level required for OMEGA EP, it was necessary to understand the root cause of this birefringence. A finite-element analysis (FEA) code (ANSYS) was used to model the stress fields induced in both square windows, such as those used in the LLNL PEPC cells, and the proposed circular windows.

FEA models of the windows were generated using 20-node quadrilateral elements with a resolution in X and Y (the plane parallel with the faces of the window) equal to 10 mm and a resolution in Z equal to 1 mm. Only one quadrant of the window was modeled because of symmetry. To better simulate edge effects, a finer mesh was used near the edges of the window. Each window was assumed to be simply supported on the perimeter of the vacuum face with a uniform pressure applied to the opposite surface. The von Mises stresses were obtained from the model at every point on the sampling mesh. Because it was found that the resulting birefringence asymptotically approached a solution with decreasing step size in Z, these stresses were linearly interpolated in Z to improve the resolution through the thickness of the window.

The Wertheim stress optic law was applied to the FEA results to predict the net birefringence.[12] By modeling the birefringent window between two ideally crossed polarizers, the passive contrast could be predicted at every point. The numerical limit for the passive contrast ratio, limited by the numerical accuracy of the FEA code, was found to be approximately 5000:1. Figure 107.4 shows model predictions for both

a square $430 \times 430 \times 35$-mm fused-silica window used in the LLNL PEPC cells and a 600-mm-diam, 40-mm-thick circular fused-silica window that was used for the LLE PEPC. In Figs. 107.4(a) and 107.4(c), 3-D maps of the magnitudes of the von Mises stresses in one quadrant of the clear aperture are shown, i.e., the region plotted in Fig. 107.4 corresponds to the black dashed square indicated in Fig. 107.2. The corresponding 2-D map of the passive contrast ratio in that same region of the square window is depicted in Fig. 107.4(b). In the case of the circular window, the calculated contrast ratio was beyond the numerical limit, and therefore no corresponding contrast ratio map is shown for this case.

The results show clearly the difference in performance between the square-window geometry and the new circular-window geometry. The model of the square window predicted a concentration of stress near the corner of the clear aperture and a resultant degradation of the contrast ratio in the corners of the clear aperture that has been reported elsewhere.[5,7] In contrast, the calculation for the circular window reveals that the model predicted no measurable degradation of the contrast ratio for this window.

This result cannot be attributed to lower stress in the circular window because the stress in the circular window was nearly 40% higher than in the square window. However, the stress in the circular window possesses a high degree of odd symmetry, with compressive stress on the air side effectively canceling the birefringence arising from the tensile stress on the vacuum side of the window. Therefore, the net birefringence experienced by the laser pulse after propagation through the entire circular window is negligible. The stresses in the square

(a)

0.6   1.7   2.8   3.9   5.0

$\times 10^6$ N/m^2

(b)   Contrast ratio

>5000

3000

1000

500

300

<100

(c)

0.8   2.3   3.8   5.3   6.8
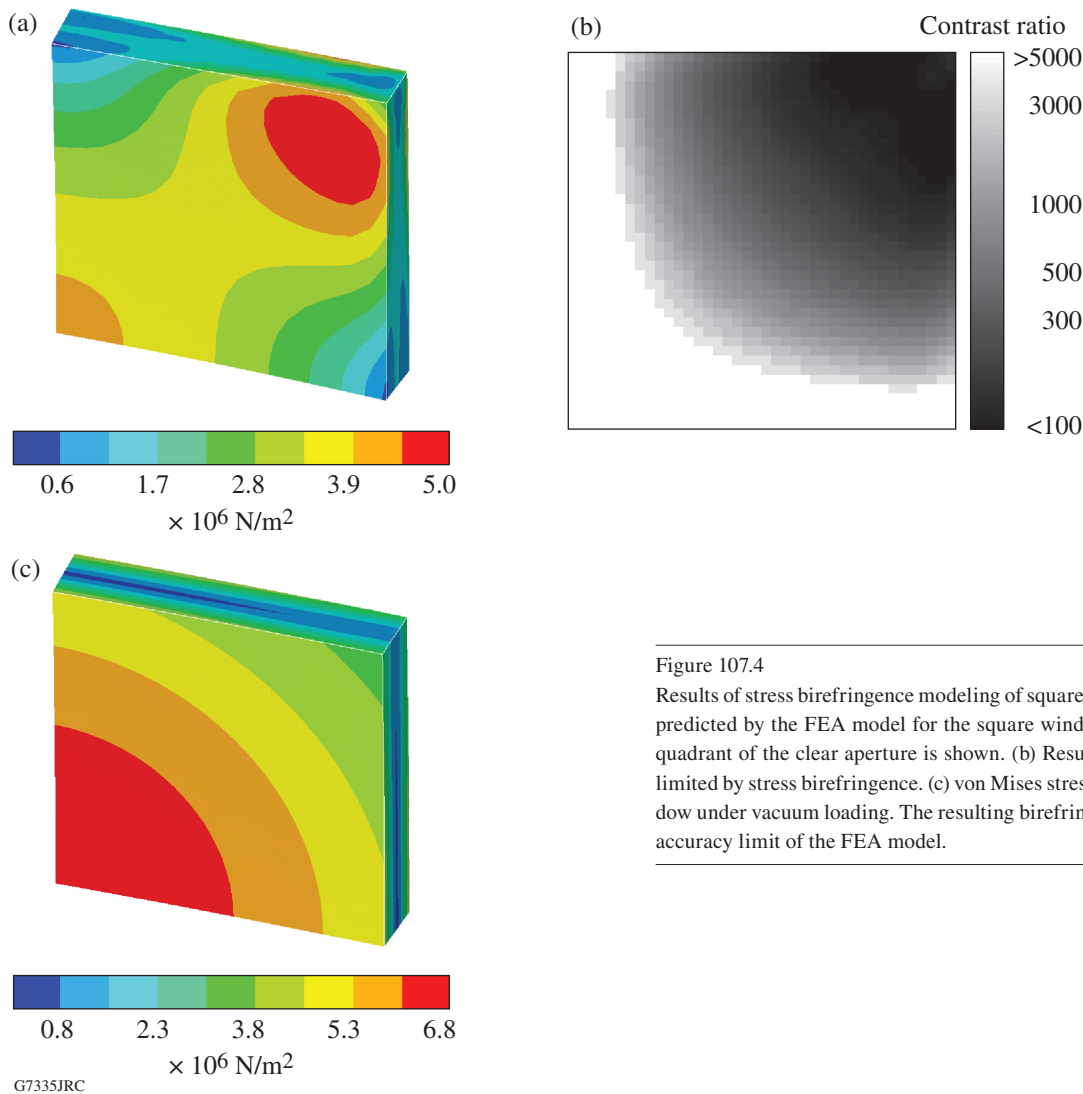
$\times 10^6$ N/m^2

G7335JRC

Figure 107.4
Results of stress birefringence modeling of square windows. (a) von Mises stresses predicted by the FEA model for the square window under vacuum loading. One quadrant of the clear aperture is shown. (b) Resulting predicted contrast ratio as limited by stress birefringence. (c) von Mises stresses predicted for a circular window under vacuum loading. The resulting birefringence was within the numerical accuracy limit of the FEA model.

window lack this degree of symmetry near the corners, where a significant retardation results. By the same logic, the result would not be expected to be significantly affected by the slightly higher thickness of the circular window, as was verified numerically.

Experimental Apparatus and Results

In this section, the characterization of the PEPC performance, the experimental testing apparatus, and a time-resolved polarimeter using a full-aperture beam is described, and the performance measured on the system is presented.

1. Full-Aperture Time-Resolved Polarimeter

The switching contrast of the PEPC was measured using the polarimeter system sketched in Fig. 107.5. A Q-switched Nd:YLF laser provided laser pulses that were sufficiently short

(<30 ns) to adequately sample the 200-ns switch pulses. The Gaussian beam was made uniform by a refractive top-hat generator, then expanded to approximately a diameter of 20 mm. A photodiode monitored the laser pulse energy and a prepolarizer fine-tuned the incident polarization to be aligned to the KDP crystal. A reflective beam expander featuring a pair of parabolic mirrors expanded the beam to a diameter of 60 cm and directed it toward the PEPC aperture.

The PEPC was mounted on a structure that allowed adjustment to the tip and tilt angles. This allowed a conoscopic alignment technique to be used to align the PEPC crystal axis to the illuminating beam.[13] The structure also allowed horizontal translation of the entire PEPC cell and enabled measurement of the obscured region.
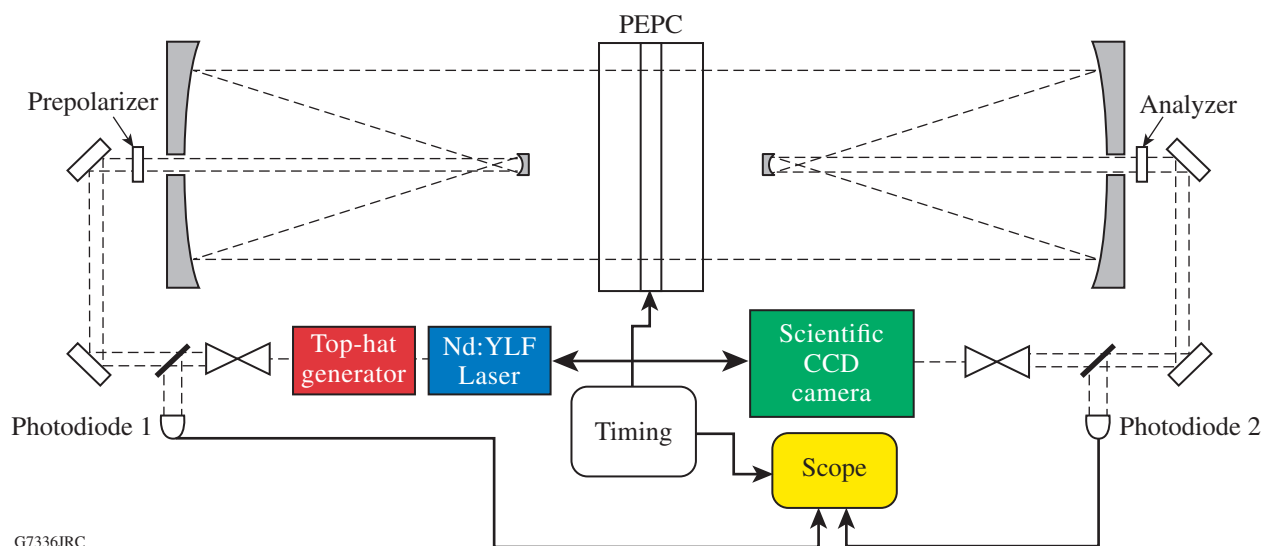
Figure 107.5
Diagram of the full-aperture polarimeter system used to test the PEPC performance.

The transmitted beam was down-collimated using an identical reflective beam expander and then passed through an analyzing polarizer. A beam sampler reflected a portion of the beam to a second photodiode. An image of the PEPC aperture was formed from the remaining beam onto a cooled 16-bit scientific CCD camera.

The laser was synchronously pulsed with the PEPC switch pulse using timing signals generated by a pulse generator. The timing system was also used to trigger an oscilloscope to capture waveform data from the photodiodes. The photodiode signals were used to measure the spatially averaged contrast over the full aperture, and the image data from the CCD camera were used to measure the contrast locally.

The contrast-ratio measurement proceeded by measuring the transmitted pulse energy with the system in a high-transmission state (or bright state) and repeating this measurement with the system in a low-transmission (dark) state. The ratio of the measurements (with background subtracted from the camera data) formed the switching contrast. To increase the dynamic range of the measurement, calibrated neutral-density filters were inserted for the bright measurements to avoid saturating the sensors while using an illumination level that would provide a measurable signal for the dark measurements. Locally, the contrast-ratio measurement is limited by the Polarcor polarizers to >10,000:1, with the minima occurring in two opposing corners of the clear aperture. Averaged over the full aperture,

contrast ratios exceeding 30,000:1 can be reliably measured. Figure 107.6 shows a local contrast map produced with no PEPC cell in the system and illustrates the measurement limit of the system. The obscuration in the center of the contrast map is due to the mounts for the two secondary mirrors.

2. Passive Contrast Results
Passive contrast measurements were conducted to assess performance limits imposed by birefringence in the PEPC windows and imperfections in the KDP crystal. They were first performed with the cell at atmospheric pressure to assess any inherent birefringence caused by dislocations in the KDP crystal or by mounting-induced stress in the fused-silica windows. The resulting contrast map is shown in Fig. 107.7(a). The minimum contrast ratio in this unloaded condition was approximately 2500:1, corresponding to a region of the window that was slightly stressed due to the window mounting. The full-aperture contrast ratio, measured using the photodiodes, was 19,800:1±1800:1, the error range being one standard deviation. Thus, the combined effects of window-mounting stress and KDP crystal imperfections were sufficiently low to achieve a local minimum contrast ratio well in excess of 1000:1.

The vacuum-loaded condition was then tested by evacuating the cell to below 100 mT and measuring the passive contrast in the same manner. The result of this measurement is shown in the contrast map in Fig. 107.7(b). In the vacuum-loaded condition, the minimum contrast ratio dropped only to ~2000:1 and
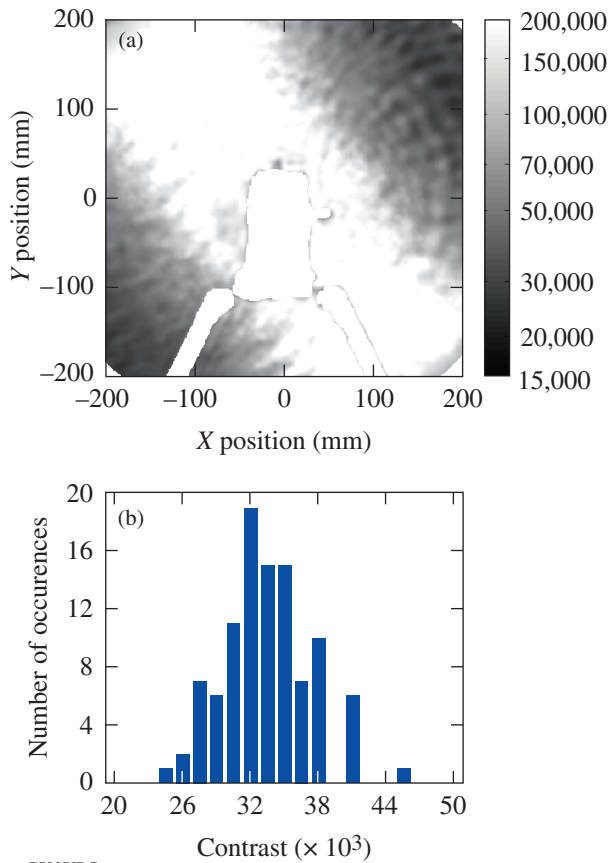
G7337JRC

Figure 107.6
Baseline passive contrast-ratio measurements performed without the PEPC cell introduced into the polarimeter, indicating the maximum measurable contrast ratio. (a) Local contrast map obtained from image data. (b) Histogram of full-aperture contrast measurements obtained from photodiode data.
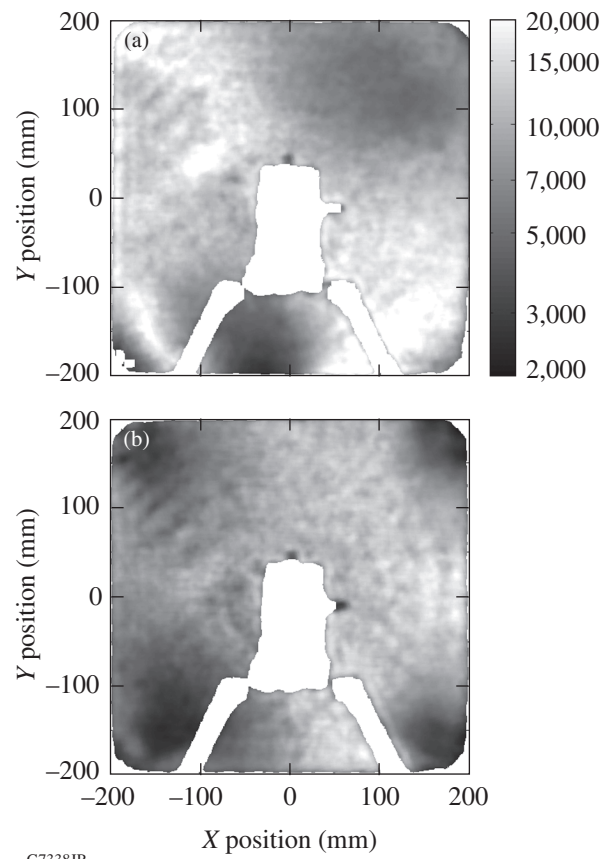

G7338JR

Figure 107.7
Passive contrast-ratio measurements performed with the PEPC cell in the polarimeter: (a) PEPC cell at atmosphere and (b) PEPC cell pumped down to <100 mT.

the full-aperture contrast was 20,400:1±1800:1. Some stress birefringence is evident, leading to a somewhat suppressed contrast ratio near the corners. The birefringence is low enough, however, to allow switching contrast well in excess of our contrast ratio requirement of >500:1.

It should be noted that in addition to using circular windows, certain other conditions are necessary to achieve this result. One requirement is that the window must be fully supported on compliant O rings. O rings are used to provide a vacuum seal around the windows and rest inside dovetail O-ring glands in the aluminum cell body. If the cross-section diameter of the O-ring material is too small, such that the O ring fully compresses into the gland under the vacuum load, the window comes into direct contact with the aluminum cell body and local stresses are formed that severely degrade the contrast ratio. This problem was alleviated by using an O ring with a sufficient diameter to

overfill the O-ring gland under vacuum loading, resulting in the window floating on top of the O ring.

3. Active Contrast Results

To assess the active-switching performance for isolating the target retroreflection at Pass 5, the prepolarizer and analyzer were aligned to each other and the laser pulse synchronized to arrive during the middle of the PEPC switch pulse [i.e., Pass 5 in Fig. 107.1(b)]. Bright-state images were obtained by setting the switch voltage to 0 V, and dark-state images were obtained with the switch voltage set to the half-wave voltage.

Figure 107.8 shows contrast results measured using this method. The surface map was generated by averaging 20 measurements acquired with the cell in three different horizontal positions. A mosaic of the three local contrast-ratio measurements was formed to minimize the obscuration from the sec-
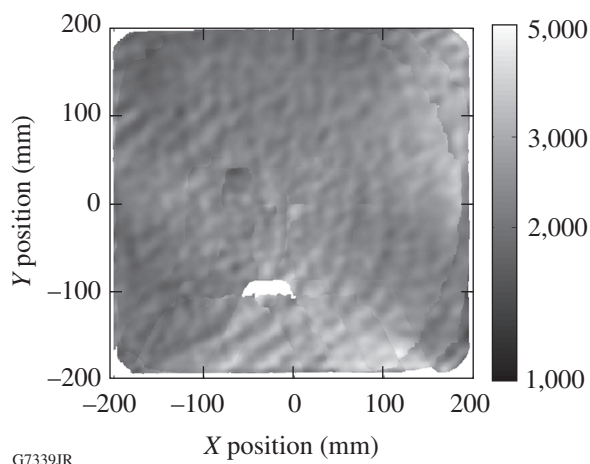
G7339JR

Figure 107.8

Map of the Pass-5 active contrast ratio measured over the clear aperture of the PEPC cell. The map was generated by overlapping three sequences of measurements with the PEPC cell in different positions laterally, thus minimizing the obscuration due to the secondary mirror mount.

ondary mirror mounts. The minimum contrast was 1390:1 in the averaged measurement, with the minimum occurring at the upper left-hand corner of the plot (corresponding to the top of the cathode side of the cell). Measuring the minimum contrast in each individual shot, the result was $\langle C_{min} \rangle$ = 1130:1±170:1. Both means of evaluating the results indicate that the 500:1 minimum contrast specification was comfortably exceeded. Over the full aperture, the contrast was 2280:1±150:1 as measured with the photodiodes.

The switching contrast corresponding to Pass 6 was also measured by setting the analyzer to the crossed position with respect to the prepolarizer for the dark-state measurements. The laser pulse timing was delayed relative to the Pass-5 measurements by 300 ns, which is the propagation time of the laser pulse from the PEPC to the deformable mirror and back into the OMEGA EP beamline. This delay places the laser pulse after the falling edge of the switch pulse, as required [see Pass 6 in Fig. 107.1(b)]. Bright-state measurements were acquired by aligning the analyzer to the prepolarizer and turning the PEPC off. The local minimum for the Pass-6 switching contrast ratio was 1010:1 based on an average of 20 measurements. The single-shot minimum contrast ratio was $\langle C_{min} \rangle$ = 1210:1±720:1. The shot-to-shot variability was higher in this experiment due to variations in the overshoot at the end of the switch pulse shape. All measured shots, however, did meet the required 500:1 specification.

4. Reliability

Having demonstrated high-contrast switching performance from the PEPC, the reliability of the system was investigated. Poor contrast during a high-energy shot presents a significant risk to system safety, and thus the PEPC must meet its contrast specification reliably.

The primary cause of intermittent failures was observed to be plasma pinching, which causes a narrow region of poor switching contrast at the top or bottom of the aperture. The frequency of this occurrence was found to be strongly dependent on the operating pressure of the cell. Figure 107.9 shows the probability of a low-contrast fringe, derived from measurements of a series of 100 PEPC shots taken at various operating pressures. The probability of a low-contrast fringe decreases exponentially with pressure, becoming negligible beyond ~70 mT. Using a gated-image intensifier, the plasma discharge during the switch pulse was observed over the range of operating pressures shown in Fig. 107.9. At low pressures (below ~40 mT), the discharge was observed to occur only along a narrow strip in the clear aperture. With increasing cell pressure, the plasma spread, eventually filling the clear aperture; on the basis of this, 80 mT was selected as the standard operating pressure.

The reliability of the cell was tested by operating the PEPC for a full day and measuring the contrast throughout the day. Figure 107.10(a) shows the results of an all-day test simulating the use conditions in OMEGA EP in which the PEPC cell
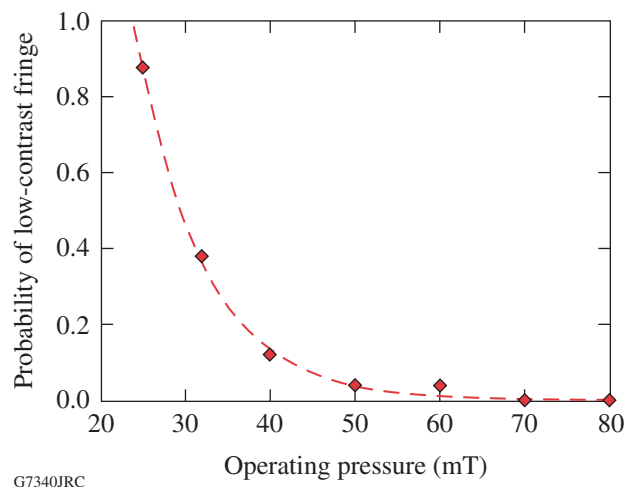

G7340JRC

Figure 107.9

Measured probability of a low-contrast fringe occurring due to locally poor plasma conductivity, as a function of operating pressure.
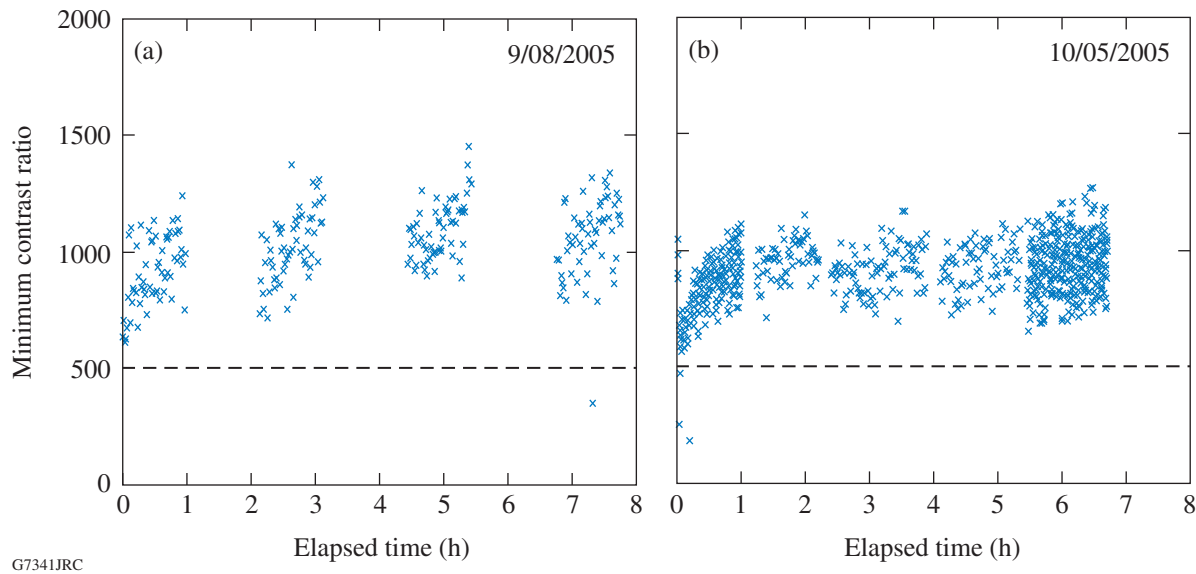
Figure 107.10
Plots of minimum local contrast ratio for individual shots during extended testing over >6 h. (a) 1-h on/off use conditions simulated and (b) PEPC run nearly continuously.

may be operated at a 1/10-Hz pulse rate for 1-h-long intervals every 2 h. In this test, the contrast was measured once per minute, although the PEPC was fired every 10 s. Of the 240 measurements that were taken during that time, one shot had a low-contrast region along the bottom edge of the clear aperture because of plasma nonuniformity. The test was repeated for continuous operation over a full day, with the results shown in Fig. 107.10(b). Images were acquired every 10 s for the first and last hours, and at 1-min intervals in between. After a 20-min warm-up period, poor shots were not observed in this test—out of over 900 measurements.

Discussion

The OMEGA EP PEPC system prototype has demonstrated that high-switching contrasts exceeding 500:1 throughout the clear aperture are obtainable using PEPC technology. The key has been the reduction of stress birefringence using circular windows. When high packing densities are required, i.e., for laser systems with a large number of closely spaced beamlines, circular windows are not feasible. This is an effective solution for systems like OMEGA EP, however, with a small number of beamlines separated by a few meters.

Work is now under way on high-contrast PEPC's for the OMEGA EP beamlines, which are currently in the integration stage. This high-contrast PEPC technology will be deployed shortly into the OMEGA EP beamlines and will provide switching and retroreflection protection for future experimental campaigns using the laser system.

REFERENCES

1. L. J. Waxer, D. N. Maywar, J. H. Kelly, T. J. Kessler, B. E. Kruschwitz, S. J. Loucks, R. L. McCrory, D. D. Meyerhofer, S. F. B. Morse, C. Stoeckl, and J. D. Zuegel, Opt. Photonics News **16**, 30 (2005).

2. G. H. Miller, E. I. Moses, and C. R. Wuest, Opt. Eng. **43**, 2841 (2004).

3. J. Goldhar and M. A. Henesian, Opt. Lett. **9**, 73 (1984).

4. M. A. Henesian and J. Goldhar, Opt. Lett. **9**, 516 (1984).

5. M. A. Rhodes *et al.*, Appl. Opt. **34**, 5312 (1995).

6. R. Bailly-Salins, C. Sudres, and J.-P. Marret, in *Third International Conference on Solid State Lasers for Application to Inertial Confinement Fusion*, edited by H. Lowdermilk (SPIE, Bellingham, WA, 1999), Vol. 3492, pp. 148–155.

7. M. A. Rhodes, S. Fochs, and P. Biltoft, Fusion Technol. **32**, 1113 (1998).

8. N. P. Zaitseva *et al.*, J. Cryst. Growth **180**, 255 (1997).

9. C. D. Boley and M. A. Rhodes, IEEE Trans. Plasma Sci. **27**, 713 (1999).

10. C. D. Boley and M. A. Rhodes, in *Solid State Lasers for Application to Inertial Confinement Fusion: Second Annual International Conference*, edited by M. L. Andre (SPIE, Bellingham, WA, 1997), Vol. 3047, pp. 672–679.

11. S. N. Fochs, M. A. Rhodes, and C. D. Boley, in *Solid State Lasers for Application to Inertial Confinement Fusion: Second Annual International Conference*, edited by M. L. Andre (SPIE, Bellingham, WA, 1997), Vol. 3047, pp. 680–691.

12. M. G. Wertheim, Comptes. Rendus Acad. Sci. Fr. **32**, 289 (1851).

13. M. J. Guardalben, Engineering and Laboratory Notes, Opt. Photonics News (Supplement), **8** (1997).